

Low energy neutron propagation in MCNPX and GEANT4

R. Lemrani^a M. Robinson^b V. A. Kudryavtsev^b M. De Jesus^c
G. Gerbier^a N. J. C. Spooner^b

^a*DAPNIA-SPP, CEA-Saclay, Gif-Sur-Yvette, France*

^b*Department of Physics and Astronomy, University of Sheffield, S3 7RH, UK*

^c*Institut de Physique Nucléaire de Lyon, IN2P3-CNRS, Université Claude Bernard Lyon-I, 4 rue Enrico Fermi, 69622 Villeurbanne Cedex, France*

Abstract

Simulations of neutron background from rock for underground experiments are presented. Neutron propagation through two types of rock, lead and hydrocarbon material is discussed. The results show a reasonably good agreement between GEANT4, MCNPX and GEANT3 in transporting low-energy neutrons.

Key words: Neutron background, Neutron flux, Neutron shielding, Spontaneous fission, (α ,n) reactions, Radioactivity, Dark matter, WIMPs

PACS: 95.35.+d, 14.20.Dh, 13.75.-n, 28.20, 25.40, 98.70.Vc

1 Introduction

Neutrons are known to be an important source of background for high sensitivity experiments searching for rare events in underground laboratories. These experiments include the direct dark matter searches, double-beta decay experiments, solar neutrino measurements etc. Significant progress has been achieved in the past few years in the development of techniques for rare event searches at different energies. This imposes more stringent restrictions on the tolerated background rates.

Dark matter direct detection experiments have developed over the last decade strong background suppression and rejection techniques. These experiments are installed in deep underground laboratories (Gran Sasso, Modane, Canfranc, Boulby, Soudan etc.) reducing cosmic ray related backgrounds by many orders of magnitude. Lead and copper shielding is used against gamma-rays.

Internal contamination is kept low by the selection of low radioactive materials. Materials implemented in the vicinity of the detectors are purified for instance by chemical or mechanical cleaning to achieve low radioactivity. Cryogenic detectors have shown a powerful event-by-event discrimination of electron and nuclear recoils [1,2,3]. Liquid noble gas detectors (see, for example, Refs. [4,5]) and other techniques are progressing towards effective gamma rejection. With the sensitivities thus achieved neutrons have become the limiting background.

Unlike other backgrounds (photons, electrons, alphas) neutrons may induce low-energy single nuclear recoils in the detectors indistinguishable from the expected WIMP signal. In underground laboratories neutrons originate overwhelmingly from the presence of uranium and thorium contaminations in the surrounding rock. Uranium and thorium produce neutrons via spontaneous fission (mainly ^{238}U) or indirectly via interactions of alphas in their decay chains with the light nuclei of the rock. Neutrons induced by cosmic-ray muon interactions with rock and shielding have much lower rate but higher probability to reach the detectors. Active veto systems will help to reject these events if necessary.

To probe the region of parameter space favoured by SUSY models a sensitivity down to at least 10^{-10} pb to the WIMP-nucleon cross-section is required. This is translated to only a few events per year per tonne of the target material in the energy range of interest. To reach such a sensitivity, the neutron background from rock, detector components and cosmic-ray muons should be significantly suppressed. For example, the neutron flux from rock should be reduced by at least 6 orders of magnitude. This can be achieved by installing passive shielding made of hydrocarbon material or water around the target. To design the shielding, its thickness, configuration and composition, Monte Carlo simulations are required. As we are talking here about several orders of magnitude reduction in the neutron flux passing through the shielding, we have to be sure that the Monte Carlo codes are accurate enough for such a job. It is therefore crucial to assess the reliability of the simulations used to design the shielding of future experiments. This paper compares for the first time propagation of neutrons through large thickness of rock and shielding using the Monte Carlo codes MCNPX [6,7] and GEANT4 [8]. Some simulations were also done with GEANT3 [9]. The calculation of the neutron production spectrum in different rocks is described in Section 2. In Section 3 the propagation of neutrons to the rock/laboratory boundary and through various shielding materials is presented. In Section 4 we compare the predictions of different Monte Carlo codes.

2 Neutron production in rock

The present study has been performed for two types of rock: NaCl, which is the rock around the Boulby Underground Laboratory hosting the ZEPLIN [4] and DRIFT [10] experiments, and the Modane rock, the Modane Underground Laboratory (LSM) being the site for the EDELWEISS [2] and NEMO-3 [11] experiments. NaCl is also the rock around the WIPP site suggested for several future experiments. There is a plan to construct another large laboratory for underground science in the Frejus tunnel which hosts the Modane laboratory. Thus the present study is relevant to several existing and future experiments and also provides important general outcomes about the code accuracy and the neutron suppression factors in the shielding.

The neutron production rates and spectra in NaCl were calculated in [12] with the SOURCES code [13]. The code determines the energy spectrum of neutrons produced in (α,n) reactions, spontaneous fission and delayed neutron emission due to radioactive isotopes present in the rock. The code uses Watt spectrum parameters, evaluated half-life and spontaneous fission branching as input for the evaluation of the spontaneous fission contribution. The (α,n) spectra assume an isotropic angular distribution in the center-of-mass system. The alpha stopping power in various media, evaluated or measured (α,n) cross-section tables and branching ratios for transitions to different excited states are used to calculate the thick target neutron yields and neutron spectra.

The code SOURCES was modified [12] to allow calculation of neutron yield from high-energy (more than 6.5 MeV) alphas. Some cross-sections were updated and more cross-sections added to the code library. The resulting spectrum assuming 60 ppb U and 300 ppb Th concentrations in NaCl is shown in Figure 1 (see also [12]).

The modified SOURCES code has also been used in the present study for the evaluation of the neutron production rate in the Modane Underground Laboratory (LSM). The LSM rock consists of glossy schist (2.65 g/cm³ density), the element concentrations (O - 50% , Ca - 31%, C - 6%, Si - 7%, Mg - 1%, Al - 2%, H - 1%, Fe - 2%) have been determined by the spectroscopy analysis [14]. New Ca and Mg cross-sections computed using the code EMPIRE [15] have been included in the SOURCES cross-section library. The concentrations of 0.84 ppm ²³⁸U and 2.45 ppm ²³²Th have been assumed in the calculation of the neutron production rate. A production rate of 1.3 neutrons/g/year has been obtained with a mean energy of 2.2 MeV (see Figure 1). Despite higher radioactivity levels for Modane rock compared to what was assumed for NaCl, the neutron production rates are very similar (1.5 neutrons/g/year in NaCl [12]). This is due to the higher (α,n) contribution per unit U/Th concentration in NaCl because of low energy thresholds for ²³Na (3.5 MeV) and ³⁷Cl (4.1

MeV), the spontaneous fission yield per unit U concentration being the same for both rocks. This results in 98% contribution of (α,n) reactions in NaCl and only 77% contribution of (α,n) reactions in the Modane rock.

3 Simulations of the neutron propagation

The neutron propagation calculations have been carried out using the MCNPX-2.5 [6,7] and GEANT4.7.0.p01 [8] simulation codes. High precision model for low-energy neutron tracking has been chosen in the GEANT4 simulations using neutron cross-section library G4NDL3.7. In MCNPX the libraries NRG-2003, la150n and JENDL [7] were used for lead, CH₂ and NaCl respectively. Some test simulations have also been run with GEANT3 [9]. Starting from the neutron production spectra provided by the SOURCES code, the neutrons have first been propagated to the rock boundary and then through different configurations of shielding. For the benchmark a simple geometry has been used, where the boundaries between different media are planar (see Figure 2).

Neutrons have been generated in a volume of rock of $1 \times 1 \text{ m}^2$ section and 3 m depth as there were essentially no neutrons crossing more than 3 metres of rock. The volume for neutron propagation has been taken much larger with a cross-section of $10 \times 10 \text{ m}^2$ and 3 m depth. This has allowed collection of all neutrons which could reach the rock/cavern boundary. Two configurations of shielding have been studied. In the first one, neutrons have been propagated through different thicknesses (5 g/cm^2 to 50 g/cm^2) of hydrocarbon shielding CH₂. In the second one, neutrons have first been propagated through a slab of lead 30 cm thick before further propagation through CH₂. Lead is commonly used in underground laboratories as gamma shielding so it was worth studying the neutron propagation in lead and its effect on the neutron flux suppression. Note that the chosen geometry is the same as used in Ref. [12] allowing direct comparison of the results. In Ref. [12] the simulations were done for NaCl with GEANT4.5.2.

All neutrons have been counted on each surface and the fluxes have been normalised to the area of 1 m^2 . In this way we can say that we counted all neutrons generated in a volume with a surface projection cross-section of 1 m^2 , that reached the surface of a medium. Other cells with the same projection cross-section will give the same neutron flux.

4 Results

Figure 3 shows the simulated neutron spectra at the surface of NaCl. The total statistics for each curve on this and subsequent graphs is at least 10^5 neutrons leading to more than 1000 neutrons per energy bin at all energies between 10 keV and 2 MeV. GEANT4, MCNPX and GEANT3 simulations differ at most by 20% in a narrow region around 1 MeV. The integrated neutron fluxes above 1 MeV agree within 10%. Note that the GEANT4 results obtained with the old cross-section library and published in Refs. [12,17] differ from the present GEANT4 simulations above 1 MeV. The difference is due to an error found in the inelastic cross-section on chlorine [18] and corrected in the present simulations. The smaller neutron flux above 1 MeV obtained with the corrected cross-section, results in smaller fluxes by about a factor of 2-3 after 20-40 g/cm² of CH₂ shielding. Agreement between GEANT4 and MCNPX for the Modane rock (Figure 4) is again fairly good, the maximal difference being about 15% around 2 MeV.

The neutron flux in the Modane rock is smaller than in NaCl despite higher U/Th concentrations and similar neutron production rates (discussed above). This is due to the presence of a small amount of hydrogen (in water) in the Modane rock and its absence in NaCl. Hydrogen serves as a good neutron moderator and the flux is very sensitive to the hydrogen abundance. Hydrogen reduces the neutron flux above 100 keV (1 MeV) at Modane by a factor 4.7 (1.8) (see also Ref. [19] for a discussion of this effect in concrete).

The neutron spectra originated in NaCl and propagated through different thicknesses of CH₂ shielding are shown in Figure 5. The agreement is satisfactory for the purpose of designing shielding. After 50 g/cm² of CH₂, MCNPX gives a differential flux 50% higher than the GEANT4 flux, translating into an additional 1-2 cm thick CH₂ layer. Figure 6 shows the corresponding integrated fluxes above 100 keV and 1 MeV. The results for GEANT4 simulations are slightly different from published in Ref. [12] due to the corrected inelastic cross-section on chlorine used in the present study. The results of neutron propagation through 30 cm of Pb and additional CH₂ layers are shown in Figures 7 and 8. Again a reasonable agreement between MCNPX and GEANT4 is observed.

To calculate accurately the real flux in a laboratory one would have to take into account the exact geometry of the cavern since the back-scattering of neutrons off the cavern walls increases the neutron flux significantly (see the discussion in Refs. [12,16]). Figure 9 shows the direct neutron flux coming from the walls of NaCl rock to the cavern with the size of $30 \times 6.5 \times 4.5$ m³ (same as in Ref. [12]) and the total flux taking into account the back-scattering of neutrons. Both GEANT4 and MCNPX predict a flux enhancement due to

back-scattering of 50% above 1 MeV. Similarly in the case of the Modane underground laboratory ($30 \times 11 \times 10 \text{ m}^3$) a flux enhancement of 32% above 1 MeV is obtained with GEANT4 and 25% with MCNPX.

5 Conclusions

We have shown the first comparison of MCNPX, GEANT4 and GEANT3 simulations of neutron propagation through different materials relevant to underground experiments. A reasonably good agreement is observed for two types of rock, lead and hydrocarbon material. The maximal observed difference in differential and integrated neutron fluxes is of the order of 50% after 50 g/cm^2 of CH_2 with MCNPX giving a flux higher than GEANT4. Keeping in mind that the flux attenuation in 50 g/cm^2 of CH_2 is about 6 orders of magnitude, such a difference does not give any reason to question the reliability of MCNPX and GEANT4 codes. This result provides a solid ground for the design of neutron shielding for experiments aiming at a background free environment. From Figures 5-8 we conclude that a neutron shielding equivalent to 55 g/cm^2 should suppress the neutron flux from environment radioactive origin by more than 6 orders of magnitude. This is roughly within the requirements for a tonne-scale dark matter experiment aiming at sensitivity of 10^{-10} pb to WIMP-nucleon spin-independent interactions [12]. Exact composition, thickness and configuration of the shielding will be determined on the basis of specific features of a particular set up. The results can also be used as a benchmark for those who would want to check their own simulations.

6 Acknowledgements

This work has been partially supported by the ILIAS integrating activity (Contract No. RII3-CT-2004-506222) as part of the EU FP6 programme in Astroparticle Physics.

References

- [1] D. S. Akerib et al. (CDMS Collaboration). *Phys. Rev. Lett.*, **93** (2004) 211301; see also astro-ph/0507190.
- [2] V. Sanglard et al. (EDELWEISS Collaboration). *Phys. Rev. D*, **71** (2005) 122002.
- [3] G. Angloher et al. *Astroparticle Phys.*, **23** (2005) 325.

- [4] G. J. Alner et al. *New Astronomy Reviews*, **49** (2005) 259.
- [5] E. Aprile et al. *New Astronomy Reviews*, **49** (2005) 289.
- [6] Briesmeister (Ed.) et al. MCNP - Version 4B (and later), *LA-12625-M*, LANL (1997).
- [7] <http://mcnpx.lanl.gov>.
- [8] S. Agostinelli et al. (GEANT4 Collaboration). *Nucl. Instrum. and Meth. In Phys. Res. A*, **506** (2003) 250.
- [9] GEANT3 Collaboration. CERN-DD/EE/84-1, September 1987.
- [10] G. J. Alner et al. Submitted to *Nucl. Instrum. and Meth. In Phys. Res. A*.
- [11] L. Simard for the NEMO Collaboration. *Nucl. Phys. B (Proc. Suppl.)*, **145** (2005) 272.
- [12] M. J. Carson et al. *Astroparticle Phys.*, **21** (2004) 667.
- [13] W. B. Wilson et al. SOURCES-4A, Technical Report *LA-13639-MS*, Los Alamos (1999).
- [14] V. Chazal et al. *Astroparticle Phys.*, **9** (1998) 163.
- [15] EMPIRE-2.19, <http://www.nndc.bnl.gov/empire219>.
- [16] P. F. Smith et al. *Astroparticle Phys.*, **22** (2005) 409.
- [17] M. J. Carson et al. *Nucl. Instrum. and Meth. In Phys. Res. A*, **546** (2005) 509.
- [18] H. M. Araújo. Personal communication.
- [19] H. Wulandari et al. *Astroparticle Phys.*, **22** (2004) 313.

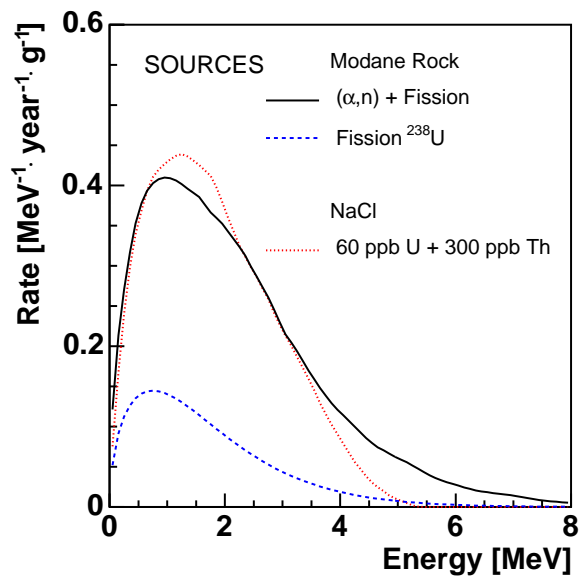


Fig. 1. Neutron energy spectrum from U and Th traces in the Modane rock simulated with SOURCES (full line) and fission contribution (dashed line). The spectrum for 60 ppb U + 300 ppb Th in NaCl is also shown (dotted line).

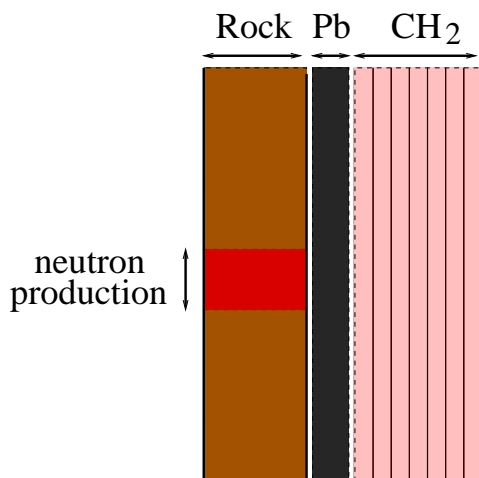


Fig. 2. Sketch of the geometry used as a benchmark for comparing the simulations.

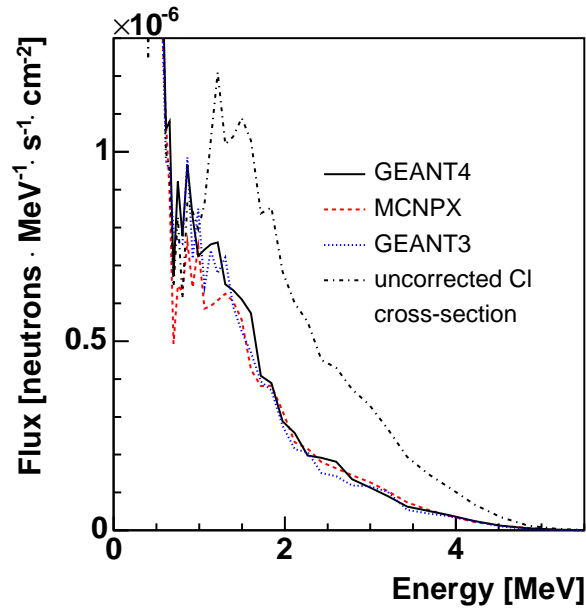


Fig. 3. Neutron energy spectra from U and Th traces in NaCl at rock boundary simulated with GEANT4 (solid line), MCNPX (dashed line) and GEANT3 (dotted line). The GEANT4 result with uncorrected inelastic cross-section is also shown (dashed-dotted line).

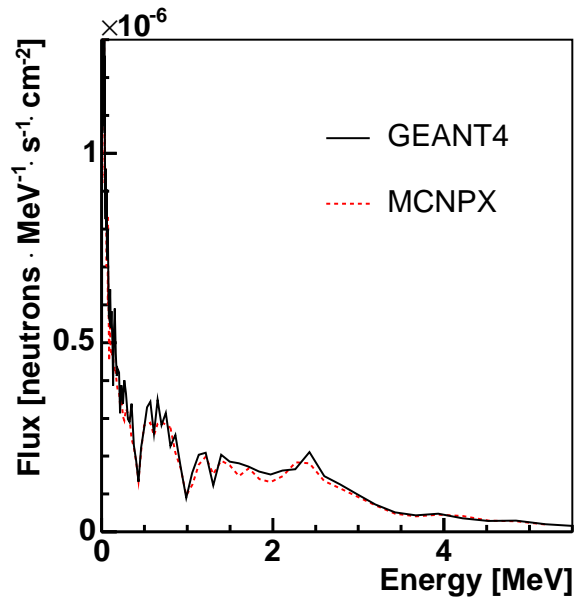


Fig. 4. Neutron energy spectra from rock activity at Modane rock boundary simulated with GEANT4 (solid line) and MCNPX (dashed line).

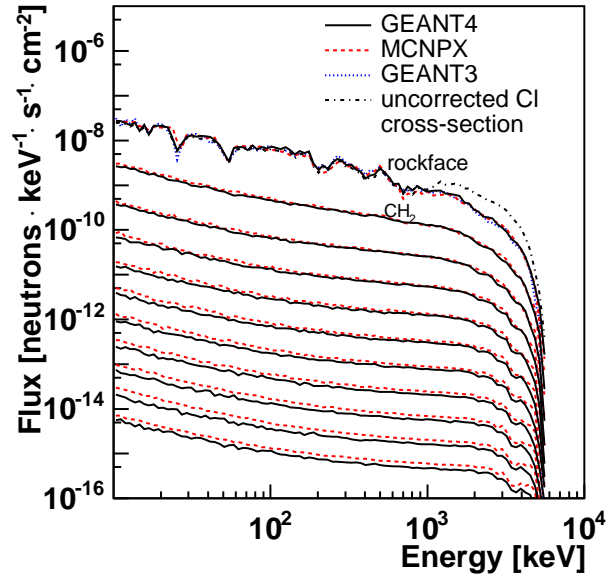


Fig. 5. Neutron energy spectra from NaCl after hydrocarbon shielding simulated with GEANT4 (solid lines) and MCNPX (dashed lines). The GEANT4 result with uncorrected inelastic cross-section is also shown (dashed-dotted line).

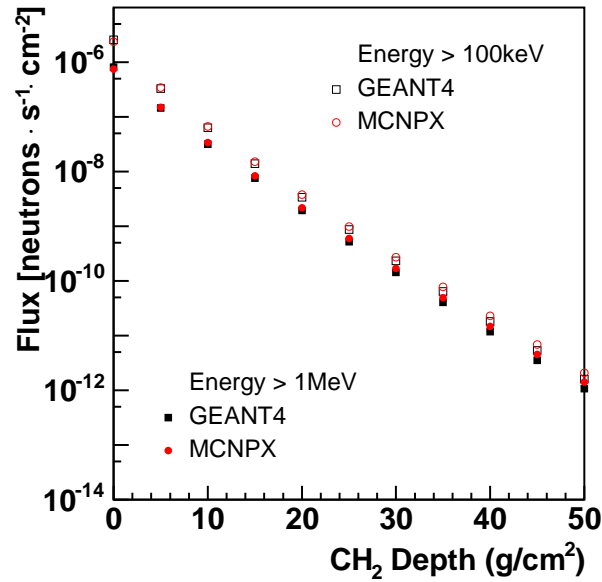


Fig. 6. Neutron flux from NaCl above 100 keV (open circles and squares) and above 1 MeV (full circles and squares) as a function of CH_2 thickness simulated with MCNPX (circles) and GEANT4 (squares).

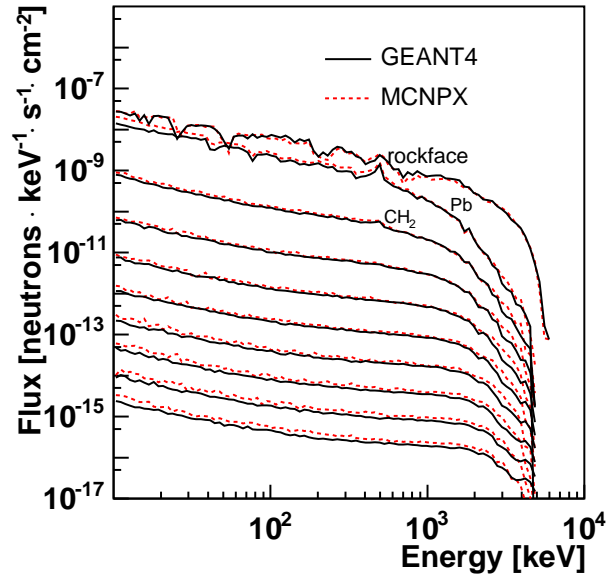


Fig. 7. Neutron energy spectra from NaCl after lead and hydrocarbon shielding simulated with GEANT4 (solid lines) and MCNPX (dashed lines).

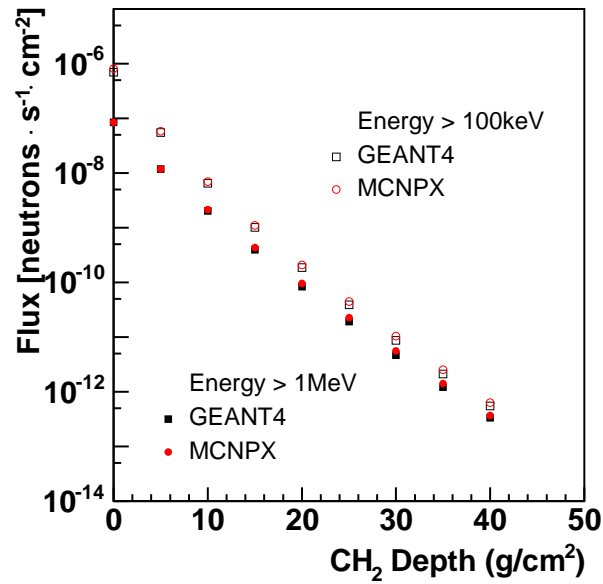


Fig. 8. Total neutron flux from NaCl above 100 keV (open circles and squares) and above 1 MeV (full circles and squares) as a function of CH_2 thickness after 30 cm of lead calculated with MCNPX (circles) and GEANT4 (squares).

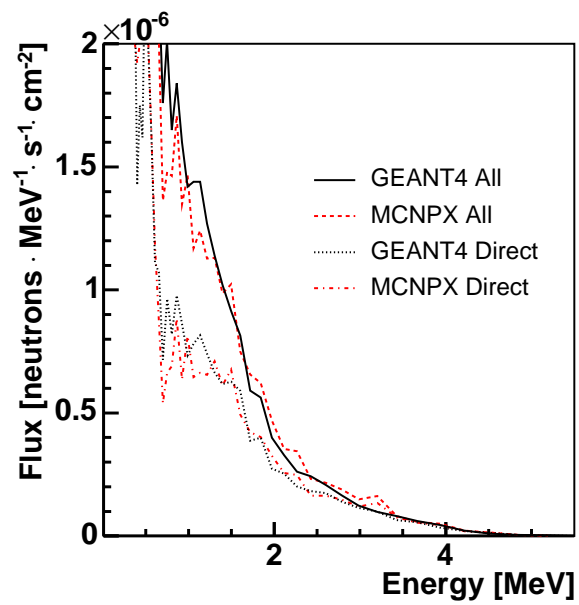


Fig. 9. Neutron energy spectra at the rock/cavern boundary from U and Th traces in NaCl taking into account back-scattering effect with GEANT4 (solid line) and MCNPX (dashed line). Also shown the direct flux (without back-scattering) with GEANT4 (dotted line) and MCNPX (dashed-dotted line).